

## Studies of forward jets and production of W, Z bosons at LHC energies

---

**K. Kutak**

*Deutsches Elektronen Synchrotron, D-22603 Hamburg, Germany*

*E-mail: kutak@mail.desy.de*

We report on application of QCD in calculations of forward jet and W, Z boson production cross sections at the Large Hadron Collider. In particular in case of jet production we emphasize dynamical features of the matrix elements controlling the resummation of logarithmically enhanced corrections in  $\sqrt{s}/E_T$ , where  $E_T$  is the jet production transverse energy. In case of production of W, Z bosons we focus on angular correlations between produced boson and hardest associated jet.

*The 2009 Europhysics Conference on High Energy Physics,  
July 16 - 22 2009  
Krakow, Poland*

## 1. Introduction

Experiments at the Large Hadron Collider (LHC) will allow to test standard model at very high energies. Here we are interested in Quantum Chromodynamics (QCD) processes like forward jet production and interplay of QCD with Electro-Weak interactions which lead to  $W$ ,  $Z$  bosons production in hadronic collision. The first of listed processes is of interest since it will allow for better understanding of partonic structure of the proton at extreme energies where new phenomena like saturation [1, 2, 3] may occur. The other process is an important candle of Electro-Weak theory which has to be tested at various energy scales in order to have full understanding of it. This process will also serve as one to calibrate calorimeters and to measure luminosities.

The large center of mass energy at the LHC will require a need to apply QCD resummation approaches capable to account for multiple scales in the problem. Namely, one has to account for logarithms of type  $\alpha_s \ln(\mu/\Lambda_{QCD})$  where  $\mu$  might be  $p_T$  of jet or mass of  $W/Z$  and logarithms coming from the fact that at least parton densities in one of the incoming proton will be probed at very small longitudinal momentum fraction  $x$  giving rise to logarithms of type  $\alpha_s^n \ln^m 1/x$ . The theoretical framework to resume consistently both kinds of logarithmic corrections in QCD calculations is based on high-energy factorization at fixed transverse momentum. [4]. This formulation depends on unintegrated distributions for parton splitting, obeying appropriate evolution equations, and short-distance, process-dependent matrix elements. The unintegrated-level evolution is given by evolution equations in rapidity, or angle, parameters. Different forms of the evolution, valid in different kinematic regions, are available, see [5, 6], and references therein, for recent work in this area and reviews. In this article we present recently obtained results for hard matrix elements needed in application of factorisation formulas for both of introduced above processes. In Sec. 2 we introduce the basic structure of jet production in the LHC forward region. In Sec. 2.1 we consider associated parton showering effects. In Sec. 2.3 we consider effects from the short-distance matrix elements that control the resummation of logarithmically enhanced corrections in  $\sqrt{s}/E_T$ , where  $E_T$  is the hard jet transverse energy. In Sec. 3 we briefly discuss central production of  $W$ ,  $Z$  bosons focusing on observables which are sensitive to different showering methods and different assumptions on initial state of colliding partons. We give concluding remarks in Sec. 4.

## 2. Forward jets

The hadroproduction of a forward jet associated with hard final state  $X$  is pictured in Fig. 1. The kinematics of the process is characterized by the large ratio of sub-energies  $s_2/s_1 \gg 1$  and highly asymmetric longitudinal momenta in the partonic initial state,  $q_A \cdot p_B \gg q_B \cdot p_A$ . At the LHC the use of forward calorimeters allows one to measure events where jet transverse momenta  $p_\perp > 20$  GeV are produced several units of rapidity apart,  $\Delta y \gtrsim 4 \div 6$  [7, 8, 9]. Working at polar angles that are small but sufficiently far from the beam axis not to be affected by beam remnants, one measures azimuthal plane correlations between high- $p_\perp$  events (Fig. 2) widely separated in rapidity [9, 10].

The presence of multiple large-momentum scales implies that, as recognized in [11, 12, 13], reliable theoretical predictions for forward jets can only be obtained after summing logarithmic

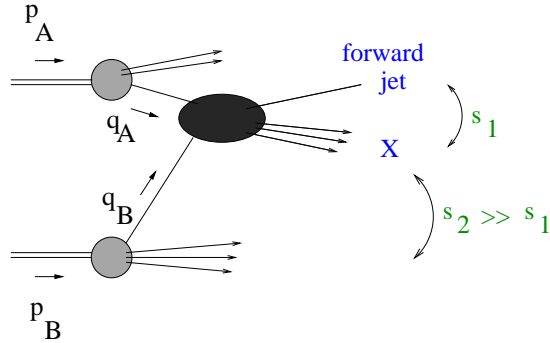


**Figure 1:** Jet production in the forward rapidity region in hadron-hadron collisions.

QCD corrections at high energy to all orders in  $\alpha_s^1$ . This motivates efforts [14, 15, 16, 17] to construct new, improved algorithms for Monte Carlo event generators capable of describing jet production beyond the central rapidity region.



**Figure 2:** (Left) High- $p_\perp$  events in the forward and central detectors; (right) azimuthal plane segmentation.

In the LHC forward kinematics, realistic phenomenology of hadronic jet final states requires taking account of both logarithms of the large rapidity interval (of high-energy type) and logarithms of the hard transverse momentum (of collinear type). The theoretical framework to resum consistently both kinds of logarithmic corrections in QCD calculations is based on high-energy factorization at fixed transverse momentum [4].

Ref. [10] investigates forward jets in this framework. It presents the short-distance matrix elements needed to evaluate the factorization formula, including all partonic channels, in a fully exclusive form. On one hand, once convoluted with the BFKL off-shell gluon Green's function according to the method of [4], these matrix elements control the summation of high-energy logarithmic corrections to the jet cross sections. They contain contributions both to the next-to-leading-order BFKL kernel [18] and to the jet impact factors [19, 20]. On the other hand, they can be used in a shower Monte Carlo generator implementing parton-branching kernels at unintegrated level (see e.g. [21, 22] for recent works) to generate fully exclusive events.

The high-energy factorized form [4, 10, 19] of the forward-jet cross section is represented in Fig. 3a. Initial-state parton configurations contributing to forward production are asymmetric, with

---

<sup>1</sup>Analogous observation applies to forward jets associated to deeply inelastic scattering [23, 24]. Indeed, measurements of forward jet cross sections at Hera [25] have illustrated that either fixed-order next-to-leading calculations or standard shower Monte Carlos [25, 26, 14], e.g. PYTHIA or HERWIG, are not able to describe forward jet  $ep$  data.

the parton in the top subgraph being probed near the mass shell and large  $x$ , while the parton in the bottom subgraph is off-shell and small- $x$ . The jet cross section differential in the final-state transverse momentum  $Q_\perp$  and azimuthal angle  $\varphi$  is given schematically by [4, 10, 19]

$$\frac{d\sigma}{dQ_\perp^2 d\varphi} = \sum_a \int \phi_{a/A} \otimes \frac{d\hat{\sigma}}{dQ_\perp^2 d\varphi} \otimes \phi_{g^*/B} , \quad (2.1)$$

where  $\otimes$  specifies a convolution in both longitudinal and transverse momenta,  $\hat{\sigma}$  is the hard scattering cross section, calculable from a suitable off-shell continuation of perturbative matrix elements,  $\phi_{a/A}$  is the distribution of parton  $a$  in hadron  $A$  obtained from near-collinear shower evolution, and  $\phi_{g^*/B}$  is the gluon unintegrated distribution in hadron  $B$  obtained from non-collinear, transverse momentum dependent shower evolution.

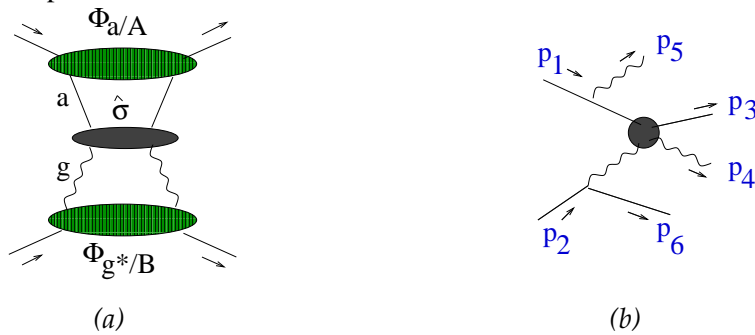


**Figure 3:** (a) Factorized structure of the cross section; (b) a typical contribution to the  $qg$  channel matrix element.

In the next section we comment on the initial-state shower evolution. In Sec. 2.2 we turn to hard-scattering contributions.

## 2.1 Parton shower evolution

Parton distributions can be obtained by parton-shower Monte Carlo methods via branching algorithms based on collinear evolution of the jets developing from the hard event [27]. The branching probability can be given in terms of two basic quantities (Fig. 4), the splitting functions at the vertices of the parton cascade and the form factors to go from one vertex to the other. An important ingredient of this approach is the inclusion of soft-gluon coherence effects [27, 28, 29] through angular ordering of the emissions in the shower.

Corrections to collinear-ordered showers, however, arise in high-energy processes with multiple hard scales [9, 30, 31], as is the case with the production of jets at forward rapidities in Fig. 1. In particular, new color-coherence effects set in in this regime due to emissions from internal lines in the branching decay chain [9, 19, 32] that involve space-like partons carrying small longitudinal momentum fractions. The picture of the coherent branching is modified in this case because the emission currents become dependent on the total transverse momentum transmitted down the initial-state parton decay chain [4, 19, 30, 31, 33]. Correspondingly, one needs to work at the level of unintegrated splitting functions and partonic distributions [5, 34] in order to take into account color coherence not only for large  $x$  but also for small  $x$  in the angular region (Fig. 5)

$$\alpha/x > \alpha_1 > \alpha , \quad (2.2)$$

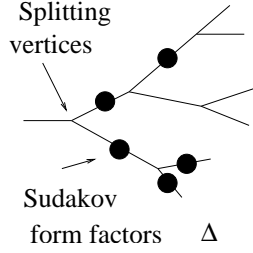


**Figure 4:** Parton branching in terms of splitting probabilities and form factors.

where the angles  $\alpha$  for the partons radiated from the initial-state shower are taken with respect to the initial beam jet direction, and increase with increasing off-shellness.

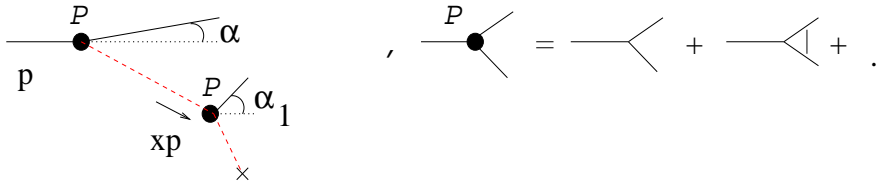


**Figure 5:** (left) Coherent radiation in the space-like parton shower for  $x \ll 1$ ; (right) the unintegrated splitting function  $\mathcal{P}$ , including small- $x$  virtual corrections.

The case of LHC forward jet production is a multiple-scale problem where coherence effects of the kind above enter, in the factorization formula (2.1), both the short-distance factor  $\hat{\sigma}$  and the long-distance factor  $\phi$ . Contributions from the coherence region (2.2) are potentially enhanced by terms  $\alpha_s^n \ln^m \sqrt{s}/p_\perp$  where  $\sqrt{s}$  is the total center-of-mass energy and  $p_\perp$  is the jet transverse momentum<sup>2</sup>. These contributions represent corrections to the angular ordering implemented in collinear showers and are not included at present in standard Monte Carlo generators [27]. Work to develop methods for unintegrated shower evolution, capable of including such corrections, is underway by several authors.

The proposal [21] incorporates NLO corrections to flavor non-singlet QCD evolution in an unintegrated-level Monte Carlo. The approach is based on the generalized ladder expansion of [35], which is extended to the high-energy region in [36]. This approach could in principle be applied generally, including flavor singlet evolution, and used to treat also forward hard processes.

## 2.2 The factorizing hard cross sections

Logarithmic corrections for large rapidity  $y \sim \ln s/p_\perp^2$  are resummed to all orders in  $\alpha_s$  via Eq. (2.1), by convoluting (Fig. 3) unintegrated distribution functions with well-prescribed short-

<sup>2</sup>Terms with  $m > n$  are known to drop out from inclusive processes due to strong cancellations associated with coherence, so that, for instance, the anomalous dimensions  $\gamma^{ij}$  for space-like evolution receive at most single-logarithmic corrections at high energy [18, 36]. This need not be the case for exclusive jet distributions, where such cancellations are not present and one may expect larger enhancements.

distance matrix elements, obtained from the high-energy limit of higher-order scattering amplitudes [10, 19]. With reference to Fig. 3b, in the forward production region we have  $(p_4 + p_6)^2 \gg (p_3 + p_4)^2$  and longitudinal momentum ordering, so that

$$p_5 \simeq (1 - \xi_1)p_1 \quad , \quad p_6 \simeq (1 - \xi_2)p_2 - k_\perp \quad , \quad \xi_1 \gg \xi_2 \quad . \quad (2.3)$$

Here  $\xi_1$  and  $\xi_2$  are longitudinal momentum fractions, and  $k_\perp$  is the di-jet transverse momentum in the laboratory frame. It is convenient to define the rapidity-weighted average  $Q_\perp = (1 - \nu)p_{\perp 4} - \nu p_{\perp 3}$ , with  $\nu = (p_2 \cdot p_4) / p_2 \cdot (p_1 - p_5)$ . In Fig. 3b Eq. (2.1) factorizes the high-energy  $qg$  amplitude in front of the (unintegrated) distribution from the splitting in the bottom subgraph. The factorization in terms of this parton splitting distribution is valid at large  $y$  not only in the collinear region but also in the large-angle emission region [4]. As a result the rapidity resummation is carried out consistently with perturbative high- $Q_\perp$  corrections [4, 19] at any fixed order in  $\alpha_s$ .

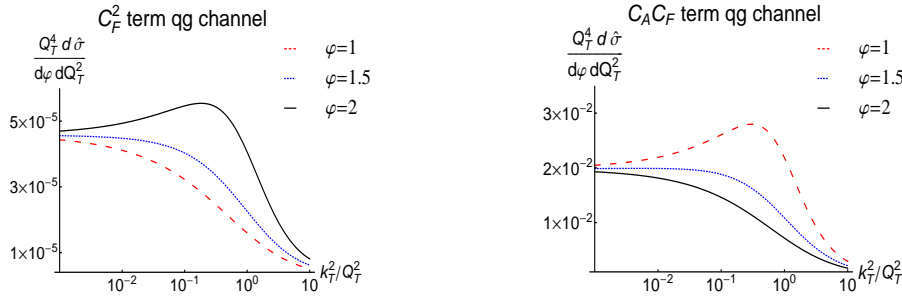


**Figure 6:** The  $k_T/Q_T$  dependence of the factorizing  $qg$  hard cross section at high energy [10]: (left)  $C_F^2$  term; (right)  $C_F C_A$  term.

The explicit expressions for the relevant high-energy amplitudes are given in [10]. Figs. 6 and 7 illustrate features of the factorizing matrix elements, partially integrated over final states. We plot distributions differential in  $Q_\perp$  and azimuthal angle  $\varphi$  ( $\cos \varphi = Q_\perp \cdot k_\perp / |Q_\perp| |k_\perp|$ ) for the case of the  $qg$  channel. Fig. 6 shows the dependence on  $k_\perp$ , which measures the distribution of the third jet recoiling against the leading di-jet system. Fig. 7 shows the energy dependence.

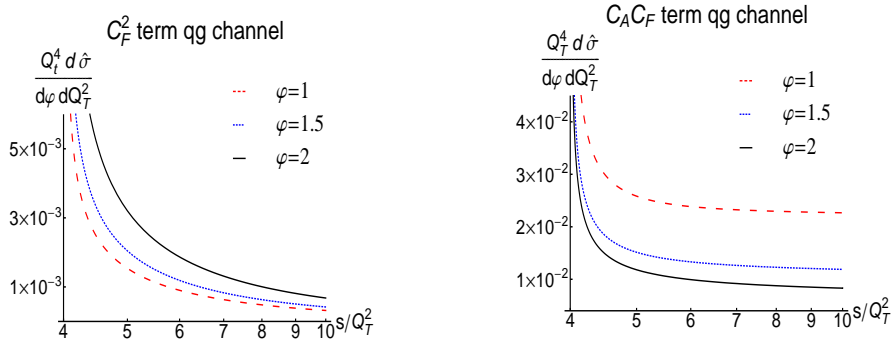


**Figure 7:** The energy dependence of the  $qg$  hard cross section [10] ( $k_T/Q_T = 1$ ).

The region  $k_\perp/Q_\perp \rightarrow 0$  in Fig. 6 corresponds to the leading-order process with two back-to-back jets. The resummation of the higher-order logarithmic corrections for large  $y \sim \ln s/p_\perp^2$

is precisely determined [4, 19] by integrating the u-pdfs over the  $k_{\perp}$ -distribution in Fig. 6. So the results in Fig. 6 illustrate quantitatively the significance of contributions with  $k_{\perp} \simeq Q_{\perp}$  in the large- $y$  region. The role of coherence from multi-gluon emission is to set the dynamical cut-off at values of  $k_{\perp}$  of order  $Q_{\perp}$ . Non-negligible effects arise at high energy from the finite- $k_{\perp}$  tail. These effects are not included in collinear-branching generators (and only partially in fixed-order perturbative calculations), and become more and more important as the jets are observed at large rapidity separations. The dependence on the azimuthal angle in Figs. 6 and 7 is also relevant, as forward jet measurements will rely on azimuthal plane correlations between jets far apart in rapidity (Fig.2).

Results for all other partonic channels are given in [10]. After including parton showering [38], quark- and gluon-initiated contributions are of comparable size in the LHC forward kinematics: realistic phenomenology requires including all channels. Note also that since the forward kinematics selects asymmetric parton momentum fractions, effects due to the  $x \rightarrow 1$  endpoint behavior [6] at the fully unintegrated level may become relevant as well.

### 3. W, Z boson production

Central production of  $W/Z$  bosons at LHC energies will be dominated by gluonic component of partonic system. The longitudinal components of incoming gluons four momenta will be small and of the same order what will result in the central production. As in the forward jet case the framework to consistently account for this kinematical set up is provided by  $k_{\perp}$  factorisation approach where  $\sigma(g^*g^* \rightarrow q(W/Z)\bar{q})$  is an off shell continuation of hard matrix element for  $\sigma(gg \rightarrow q(W/Z)\bar{q})$  [39, 40] which allows to include effects coming from finite transversal momenta of gluons. The interesting observable to calculate for this production process is the angular distance between highest  $p_{\perp}$  jet and  $p_{\perp}$  of  $Z$  or  $W$ , which allows for estimation of uncertainties of theoretical predictions. On Fig. 9 (left) we show comparison of calculation based on  $k_{\perp}$  factorisation approach [39, 40] and collinear approach at LO and NLO. We see that the distributions are considerably different for small angles in case of  $k_{\perp}$  factorisation approach and collinear LO. While NLO collinear is quite similar to the one obtained in  $k_{\perp}$  factorisation approach. The reason for that comes from the momentum conservation in LO collinear approach which forbids events in region from 0 to  $\pi/2$ . This not the case in  $k_{\perp}$  factorisation approach and NLO collinear calculation where the additional transversal momentum flow allows momenta of  $Z$ ,  $b$  and  $\bar{b}$  to be unbalanced. The  $k_{\perp}$  factorisation formula while applied to this process takes form:

$$\sigma = \phi_{a^*/A} \otimes \widehat{\sigma}(g^*g^* \rightarrow q(W/Z)\bar{q})\phi_{b^*/B} , \quad (3.1)$$

The other important distribution is the differential cross section in the transversal momentum of  $Z$   $b\bar{b}$  system 9 (right). This distributions are rather different at small  $p_{Zb\bar{b}\perp}$  region. The difference is due to the fact that in the  $k_{\perp}$  factorisation approach subleading terms of all orders from point of view of collinear approach are taken into account. We also see that at higher values of  $p_{Zb\bar{b}\perp}$  both approaches agree.

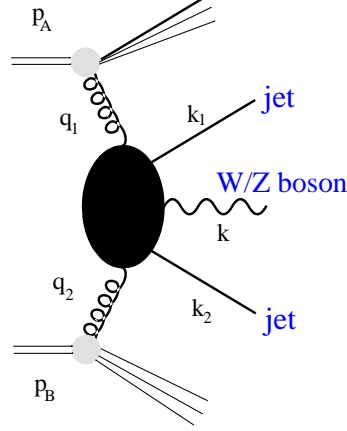


**Figure 8:** Jet production in the forward rapidity region in hadron-hadron collisions.

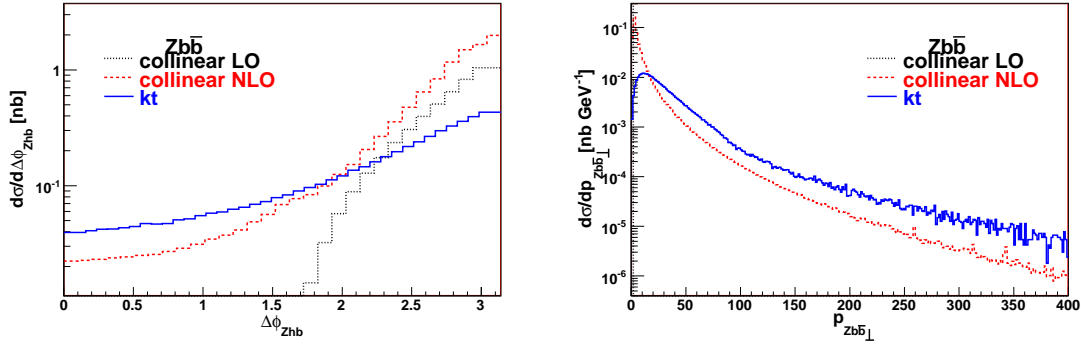


**Figure 9:** Distributions of the distance in azimuthal angle of Z and highest  $p_{\perp}$  quark or antiquark. Calculation with massive  $b$ -quarks (left). Comparison of cross sections in transverse momentum of the produced Z gauge boson. Calculation with massless  $b$ -quarks (right)

## 4. Conclusions

Forward + central detectors at the LHC allow jet correlations to be measured across rapidity intervals of several units,  $\Delta y \gtrsim 4 \div 6$ . Such multi-jet states can be relevant to new particle discovery processes as well as new aspects of standard model physics. Existing sets of forward-jet data in ep collisions, much more limited than the potential LHC yield, indicate that neither conventional parton-showering Monte Carlos nor next-to-leading-order QCD calculations are capable of describing forward jet phenomenology. Improved methods to evaluate QCD predictions are needed to treat the multi-scale region implied by the forward kinematics. In this article we have discussed ongoing progress, examining in particular factorization properties of multi-parton matrix elements in the forward region, and prospects to include parton-showering effects with gluon coherence not only in the collinear region but also in the large-angle emission region. We also have discussed predictions for W and Z central production based on different showering schemes.



## Acknowledgments

I thank the conference organizers and the conference staff for the nice atmosphere at the meeting. The results presented in Sec. 2 of this article have been obtained in collaboration with M. Deák, F. Hautmann and H. Jung while the results presented in Sec.3 were obtained by M. Deák and F. Schwennsen

## References

- [1] L. V. Gribov, E. M. Levin and M. G. Ryskin, *Phys. Rep.* **100** (1983) 1; I. I. Balitsky, *Nucl. Phys.* **B463** (1996) 99; Y. V. Kovchegov, *Phys.Rev* **D60** (1999) 034008; J. Kwiecinski, K.Kutak *Eur.Phys.J.* C29:521,2003; J. Bartels, K. Kutak *Eur.Phys.J.* C53:533-548,2008; J. L. Albacete, N. Armesto, J. G. Milhano, C. A. Salgado, U. A. Wiedemann *Phys.Rev.* D71 (2005) 014003; C. Marquet, G. Soyez *Nucl.Phys* A760 (2005) 208-222; K. Kutak, *Phys.Lett.* B675:332-335,2009
- [2] E. Iancu, M.S. Kugeratski and D.N. Triantafyllopoulos, *Nucl. Phys.* **A808** (2008) 95; Y. Hatta, E. Iancu and A.H. Mueller, *JHEP* **0801** (2008) 026; E. Iancu, C. Marquet and G. Soyez, *Nucl. Phys.* **A780** (2006) 52; C. Marquet and R. B. Peschanski, *Phys. Lett.* **B587** (2004) 201.
- [3] D. d'Enterria, *Eur. Phys. J. A* **31** (2007) 816; S. Cerci and D. d'Enterria, arXiv:0812.2665.
- [4] S. Catani, M. Ciafaloni and F. Hautmann, *Phys. Lett.* **B307** (1993) 147; *Nucl. Phys.* **B366** (1991) 135; *Phys. Lett.* **B242** (1990) 97.
- [5] J.C. Collins, hep-ph/0106126, in Proc. Workshop DIS01; arXiv:0808.2665 [hep-ph], in Proc.
- [6] F. Hautmann, *Phys. Lett.* **B655** (2007) 26; arXiv:0708.1319; J.C. Collins and F. Hautmann, *JHEP* **0103** (2001) 016; *Phys. Lett.* **B472** (2000) 129.
- [7] CMS Coll., CERN-LHCC-2006-001 (2006); CMS PAS FWD-08-001 (2008).
- [8] X. Aslanoglou et al., CERN-CMS-NOTE-2008-022 (2008); *Eur. Phys. J. C* **52** (2008) 495.
- [9] H. Jung et al., Proc. Workshop "HERA and the LHC", arXiv:0903.3861 [hep-ph].
- [10] M. Deák, F. Hautmann, H. Jung and K. Kutak, *JHEP*09(2009) 121.
- [11] A.H. Mueller and H. Navelet, *Nucl. Phys.* **B282** (1987) 727.
- [12] V. Del Duca, M.E. Peskin and W.K. Tang, *Phys. Lett.* **B306** (1993) 151.
- [13] W.J. Stirling, *Nucl. Phys.* **B423** (1994) 56.
- [14] C. Ewerz, L.H. Orr, W.J. Stirling and B.R. Webber, *J. Phys.* **G26** (2000) 696; J. Forshaw, A. Sabio Vera and B.R. Webber, *J. Phys.* **G25** (1999) 1511.
- [15] L.H. Orr and W.J. Stirling, *Phys. Lett.* **B436** (1998) 372.
- [16] J.R. Andersen, V. Del Duca, S. Frixione, F. Maltoni, C.R. Schmidt and W.J. Stirling, hep-ph/0109019; J.R. Andersen, V. Del Duca, S. Frixione, C.R. Schmidt and W.J. Stirling, *JHEP* **0102** (2001) 007.
- [17] J.R. Andersen, arXiv:0906.1965 [hep-ph], J.R. Andersen and A. Sabio Vera, *Phys. Lett.* **B567** (2003) 116.
- [18] V.S. Fadin and L.N. Lipatov, *Phys. Lett.* **B429** (1998) 127; G. Camici and M. Ciafaloni, *Phys. Lett.* **B430** (1998) 349.
- [19] M. Ciafaloni, *Phys. Lett.* **B429** (1998) 363.

- [20] F. Schwennsen, hep-ph/0703198; J. Bartels, A. Sabio Vera and F. Schwennsen, arXiv:0709.3249, JHEP **0611** (2006) 051; J. Bartels, D. Colferai and G.P. Vacca, Eur. Phys. J. **C24** (2002) 83.
- [21] S. Jadach and M. Skrzypek, arXiv:0905.1399 [hep-ph].
- [22] F. Hautmann and H. Jung, JHEP **0810** (2008) 113; arXiv:0804.1746 [hep-ph].
- [23] A.H. Mueller, Nucl. Phys. B Proc. Suppl. **18C** (1990) 125.
- [24] W.K. Tang, Phys. Lett. **B278** (1992) 363; J. Bartels, A. De Roeck and M. Loewe, Z. Phys. **C54** (1992) 635; J. Kwiecinski, A.D. Martin and P.J. Sutton, Phys. Rev. **D46** (1992) 921; S. Catani, M. Ciafaloni and F. Hautmann, Nucl. Phys. B Proc. Suppl. **29A** (1992) 182.
- [25] A. Aktas et al., Eur. Phys. J. **C46** (2006)27; S. Chekanov et al., Phys. Lett. **B632** (2006)13.
- [26] B.R. Webber, hep-ph/9510283, in Proc. Workshop DIS95.
- [27] B.R. Webber, *CERN Academic Training Lectures* (2008).
- [28] Yu.L. Dokshitzer, V.A. Khoze, A.H. Mueller and S.I. Troian, *Perturbative QCD*, Ed. Frontieres, Gif-sur-Yvette (1991).
- [29] M. Ciafaloni, in *Perturbative Quantum Chromodynamics*, ed. A.H. Mueller (World Scientific, Singapore, 1989)
- [30] G. Marchesini and B.R. Webber, Nucl. Phys. **B386** (1992) 215.
- [31] B. Andersson et al., Eur. Phys. J. **C 25** (2002) 77.
- [32] B. Andersson, G. Gustafson and J. Samuelsson, Nucl. Phys. **B467** (1996) 443.
- [33] H. Jung, Mod. Phys. Lett. **A 19** (2004) 1.
- [34] F. Hautmann and H. Jung, Nucl. Phys. Proc. Suppl. **184** (2008) 64 [arXiv:0712.0568 [hep-ph]]; arXiv:0808.0873 [hep-ph]; F. Hautmann, Acta Phys. Polon. **B 40** (2009) 2139.
- [35] G. Curci, W. Furmanski and R. Petronzio, Nucl. Phys. **B175** (1980) 27.
- [36] S. Catani and F. Hautmann, Nucl. Phys. **B427** (1994) 475; Phys. Lett. **B315** (1993) 157.
- [37] M. Ciafaloni and D. Colferai, JHEP **0509** (2005) 069; M. Ciafaloni, D. Colferai, G.P. Salam and A.M. Stasto, Phys. Lett. **B635** (2006) 320; G. Altarelli, R.D. Ball and S. Forte, arXiv:0802.0968 [hep-ph].
- [38] M. Deák, F. Hautmann, H. Jung and K. Kutak, in preparation.
- [39] M. Deák, F. Schwennsen, JHEP **0809** (2008) 035;
- [40] S.P. Baranov, A.V. Lipatov, N.P. Zotov Phys. Rev. **D78** (2008) 014025.